Selected Supersonic Combustion Activities at DLR within the European LAPCAT Project

O.J. Haidn, H.K. Ciezki*, K. Hannemann**, S. Karl***
DLR – German Aerospace Center
** Institute of Space Propulsion*
Lampoldshausen, Langer Grund, D-74239 Hardthausen, Germany
***Institute of Aerodynamics and Flow Technology*
Bunsenstr. 10, D-37073 Göttingen, Germany

Abstract
Within the LAPCAT project the working areas of the DLR Institute of Space Propulsion at Lampoldshausen and of the DLR Institute of Aerodynamics and Flow Technology at Göttingen/Braunschweig are focussed on basic experimental and numerical investigations of scramjet combustor processes with regard to the engine development for a proposed Mach 8 long distance cruise plane. The present paper gives an overview of the conducted work and the results, which have been obtained up to now. They cover the investigation of the performance characteristics of single injectors with different outer shapes with regard to mixing and combustion enhancement in a connected tube facility and experimental and numerical investigations of the performance characteristics of a complete scramjet flight test configuration consisting of intake, combustor and exhaust in a free jet ground based test facility.

1. Introduction

One of the aims of the development of future air transport systems focuses on a significant reduction of travelling times. Within the LAPCAT program[1] (Long-Term Advanced Propulsion Concepts and Technologies), which is funded by the European community, technologies for advanced propulsion concepts are investigated which are required in order to allow a potential reduction of the travelling time of long-distance flights, e.g. Brussels to Sydney, to about 2 to 4 hours. At flight speeds of 4 - 8 times the speed of sound, classical turbo-jet engines need to be replaced by advanced air-breathing engines or combinations between rocket and air-breathing engines. Although significant advances have been made in developing scramjet engines, including the University of Queensland's supersonic combustion flight experiment HyShot[2], performed in July 2002 and the flight of NASA's X-43 in March 2004[3], major scientific and technological challenges remain.
The subject of the LAPCAT project of the 6th European Framework Program is the development of key technologies for advanced high speed air-breathing propulsion systems. The selected research activities conducted in the framework of this project that are presented in the present paper are part of the scramjet research activities performed at the DLR institutes of Space Propulsion and of Aerodynamics and Flow Technology. Due to the complexity of the flows in the propulsion systems of advanced hypersonic transport vehicles, a strong link between ground based experiments, flight testing and computational fluid dynamics is needed to improve the understanding of flow phenomena, which are relevant to increase combustion efficiency and to reduce skin friction in scramjet engines. The scramjet research activities of the DLR Institute of Space Propulsion focus mainly on experimental activities on supersonic combustion in the connected tube facility M11. The main goal of these experiments is the detailed investigation of combustion characteristics and the performance of different injectors. The contributions from the Institute of Aerodynamics and Flow Technology include the numerical and experimental investigation of the complete HyShot[2] supersonic combustion flight configuration in the High Enthalpy Shock Tunnel Göttingen, HEG.

2. Investigation on single injector characteristics in the connected tube facility M11

The DLR institute of Space Propulsion at Lampoldshausen has a long experience in the investigation of mixing and combustion processes within scramjet model combustors, see e.g. [4-7]. The objective of the task within the LAPCAT program was to show the influence of the outer shape of two different injectors on the combustion chamber flow with respect to mixing enhancement and pressure increase by combustion heat release in the compressible flow. Furthermore the obtained experimental data shall serve as a test case and reference for numerical calculations and code verification within the LAPCAT project.
The scramjet combustor experiments were conducted at the M11-4 test bench of the M11 test complex. The test bench was made up of an air heater at which various experimental setups can be mounted. The air heater is able to produce hot air under pressure with total temperatures of up to $T_{t,air}$=1500 K by using H_2/O_2-burners. The oxygen mole fraction of the hot gas flow was kept constant at 21 % by adding additional oxygen. The hot vitiated air was then expanded through a Mach 2 Laval nozzle into the actual model scramjet combustion chamber.
One of the two hydrogen injectors, which are subject to this study, was installed horizontally at a time, spanning the combustion chamber from the left to the right side wall as can be seen in the sketches of Fig. 1. The injector nozzles were designed to introduce the gaseous hydrogen at a Mach number M_{H2}=2.3 into the Mach 2 air flow. The combustor entrance cross section had a width of 40 mm and a height of 50 mm. The combustion chamber width was kept constant. After 38 mm of constant chamber height the top and bottom walls had a 3° opening angle to avoid thermal choking in reacting flow conditions. Windows were located on both side walls as well as on the top and bottom walls of the combustor for optical access. This allowed application of various optical diagnostic tools to the flow field and combustion process over the entire length of the model combustor. Various experimental techniques such as Particle Image Velocimetry (PIV), Laser-Induced Florescence (PLIF), spontaneous OH-emission, etc. were used. Only a few selected results are presented here due to limited space.

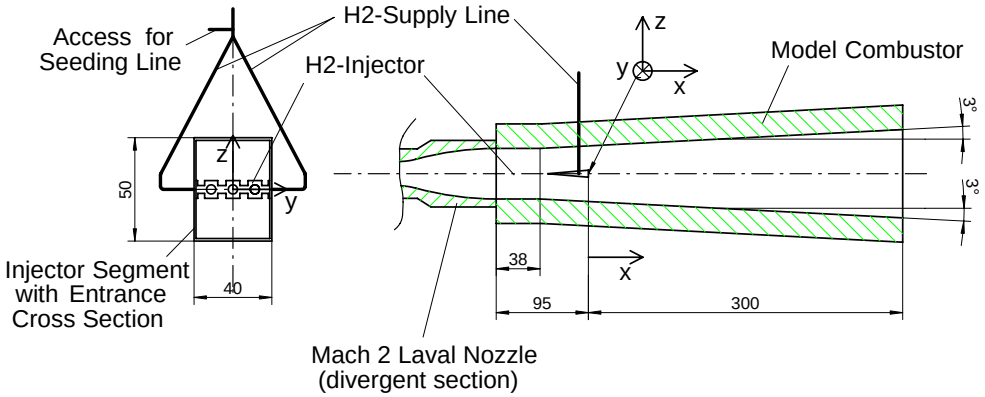

Figure 1: Scramjet model combustion chamber with installed injector.

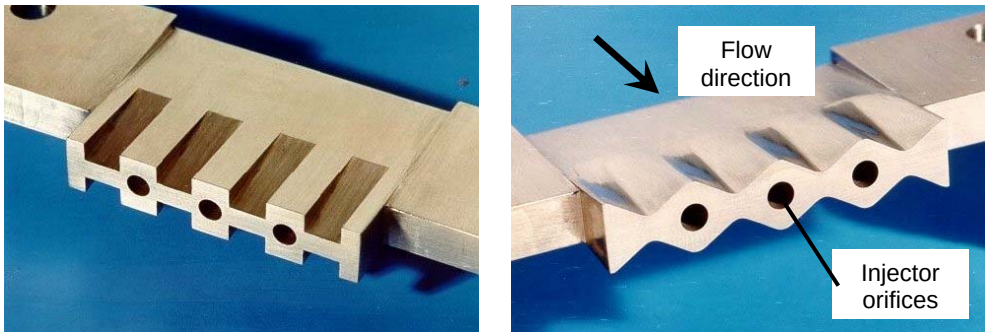

Figure 2: Studied injectors; left: USCER injector; right: WAVE injector.

Both studied injectors are wedge injectors and differ with respect of their outer shape as can be seen on the images of Fig. 2. They were designed to produce gradients of static pressure, density and flow velocity over their surface, normal to the main flow direction. These gradients lead to downstream vortices, which are known to cause mixing enhancement. The USCER injector (left image of Fig. 2) exhibits compression ramps and expansion ramps (or expansion troughs) both on the top and the bottom surface, creating areas of relatively compressed flow over the

ramps and relatively expanded flow through the troughs. The thus created gradients in velocity, static pressure and density, which are oriented normal to the main flow direction, lead to downstream oriented vortices. The WAVE injector, in contrast to the USCER injector, has no such sharp geometrical discontinuities to produce the streamwise vortices. But also the wave shaped surface geometry causes gradients normal to the main flow direction of the above described kind. For detailed information concerning the test facility, the used injectors and the test conditions, see Refs. [8,9].

Figure 3 presents the static wall pressure distributions at the top wall along the combustion chamber x-coordinate for both injectors at two different air flow conditions. In test case TC1 an air total temperature $T_{t,air}$=1300 K and in TC2 a higher temperature $T_{t,air}$=1400 K were used. The origin of the x-co-ordinate is located at the base of the injectors and constitutes the combustion chamber center line as can be seen in the sketches of Fig. 1. The pressure traces can be correlated with the positions of the trains of shock and expansion waves, which are e.g. visible on Schlieren images. The left diagram shows the data from experiments with the lower air total temperature $T_{t,air}$=1300 K, where no chemical reaction was observed. The pressure traces of both injectors are similar over the whole measured range, which indicate similar flow fields. The pressure traces at the higher air total temperature $T_{t,air}$=1400 K (TC2) of both injectors, however, where combustion occurs, are quite similar only up to ca. x≈60 mm as can be seen in the right diagram of Fig. 3. Downstream the second maximum higher pressure values were measured for the WAVE injector in comparison to the USCER injector. This pressure difference becomes even larger downstream of the third maximum at x≈170 mm. Also the second pressure maximum at ca. x=70 mm of the WAVE injector pressure trace is broader than for the USCER injector.

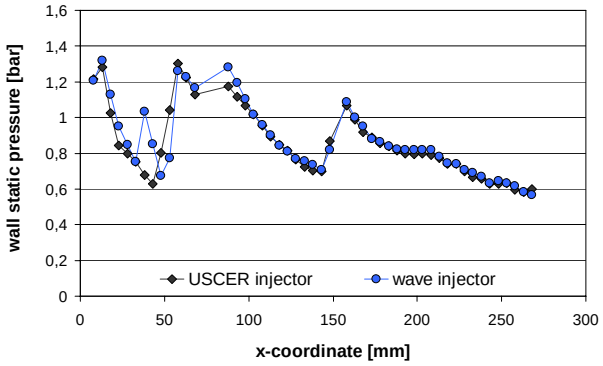

TC1 (non-reacting ("cold") test case, $T_{t,air}$=1300 K). Data points are averaged over experiment duration.

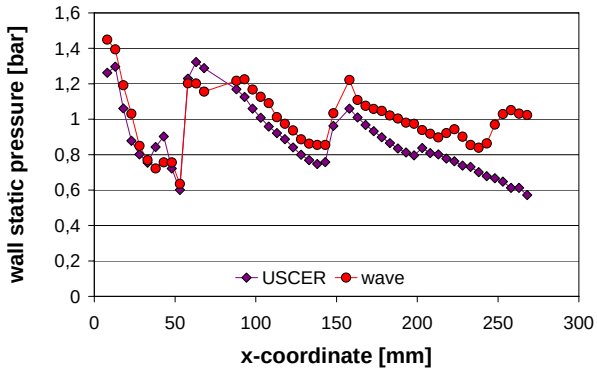

TC2 (reacting test case, $T_{t,air}$=1400 K). Data points are taken at experiment elapsed time t=3.224 s.

Figure 3: Wall static pressure distribution at top wall for USCER and WAVE injectors; $T_{t,H2}$=300 K, $\dot{m}_{H2}$ =12 g/s.

For the determination of the mixing characteristics of both injectors a Mie scattering setup with a KrF-Excimer laser emitting at a wavelength of λ=248 nm together with a ICCD camera was applied. The emitted light was formed into a light sheet and guided to traverse the combustion chamber from top to bottom in the x-z-plane at y=0 mm (center plane) and y=-5 mm (halfway in between two injector nozzles). The hydrogen jet was seeded with Aerosil R812 particles to enhance the contrast between the H_2 jet and the surrounding air flow. From the obtained Mie scattering images, profiles of measured scattering intensity were evaluated at various x-co-ordinates in order to determine the H_2 jet thickness. This was determined to be the extension of the intensity profile at the point, where half the maximum intensity was measured, resulting in D_{FWHM} (full width at half maximum).

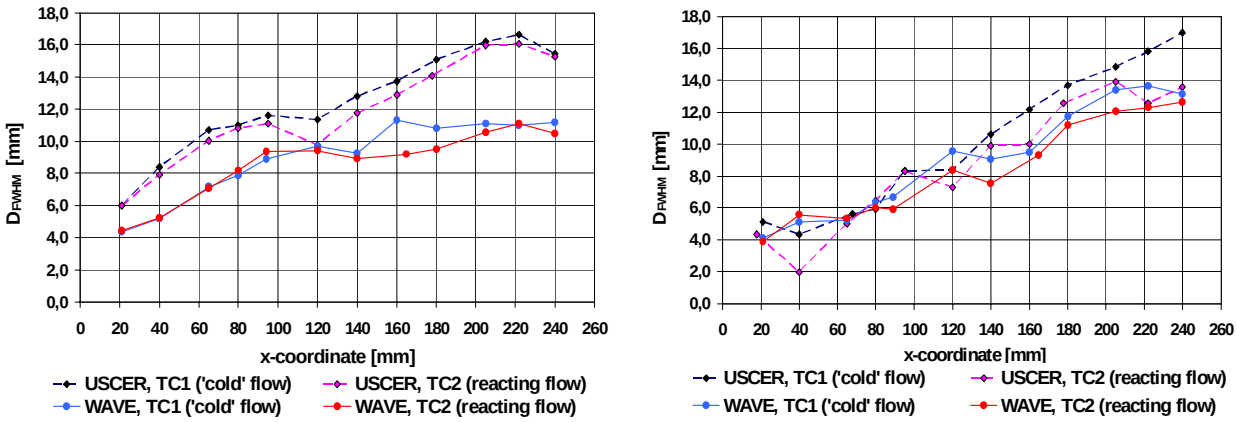

Figure 4: Growth of D_{FWHM}; left: center plane at y=0 mm; right: measuring plane at y=-5 mm.

Fig. 4 presents the hydrogen jet thickness D_{FWHM} in the two measuring planes for both injectors and for both test conditions TC1 and TC2. The diagrams reveal that injection from the USCER injector results in larger D_{FWHM} at both measurement planes. It is also obvious that D_{FWHM} is smaller for the reacting flow condition than for the pure mixing flow of TC1. Also can be seen on the right diagram (at y=-5 mm) that the D_{FWHM} growth rates of both injectors have strong similarities. Up to x≈120 mm similar jet thickness D_{FWHM} values have been measured for both injectors, while downstream the USCER injector shows noticeably higher values. According to these measurements it is likely that the hydrogen-air-interface caused by the USCER injector is more convoluted in the near field of the injection while being rather flat in the far field and vice versa when installing the WAVE injector. Thus this convolution in the second half of the combustor seems to favor a rapid heat release as could be observed when using the WAVE injector.
Summarizing can be said that the obtained results show that the outer shape of the investigated hydrogen injectors has a distinct influence on the mixing and combustion process inside the model scramjet combustor. Laser diagnostic measurements of the extension of the hydrogen jet delivered indications that for the WAVE injector a more favourable 3-dimensional structure of the hydrogen-air-interface and mixing layer was created, resulting in a noticeably higher heat release in the reacting flow case.

3. Experimental an numerical investigation of the HyShot supersonic combustion flight configuration in HEG

3.1. Scope of the investigation

Within the LAPCAT project experimental and numerical analysis of the HyShot supersonic flight experiment configuration is carried out. The experimental investigations utilizing a 1:1 scale wind tunnel model of the fuelled side of the flight configuration are currently carried out in the DLR High Enthalpy Shock Tunnel Göttingen, HEG. In the first phase of LAPCAT, the experimental data of the HyShot post flight analysis conducted in the framework of the ESA Technology Research Program "Evaluation of Full-Engine Scramjet Technology" was used for designing a new wind tunnel model with improved spatial resolution of pressure and heat flux measurements and allowing high speed flow visualisation. Further, this data was used for validation of the models implemented in the DLR TAU code to numerically describe laminar and turbulent combustion processes. The results of the HyShot post flight analysis in HEG show qualitative good agreement with the flight data and confirm the establishment of supersonic combustion. The experimental setup, applied measurement techniques and results are described in detail by Gardner et al.[10]. The numerical activities within LAPCAT accompanying the preparation and performance of the experimental activities in HEG include the application of the DLR flow solver TAU [11] to determine the free stream conditions in the HEG test section, to compute the HyShot intake flow field and the calculation of the 3-dimensional turbulent reacting flow in the HyShot combustor. The experimental and numerical results presented in this paper correspond to the HEG condition XII which duplicates the HyShot free stream conditions at a flight altitude of 32.5 km.

3.2. Numerical model

All numerical investigations within this study were performed with the hybrid structured/unstructured DLR Navier-Stokes solver TAU[11], which is validated for a wide range of steady and unsteady sub-, trans- and hypersonic flow cases. The TAU code is a second order finite-volume flow solver for the Euler and Navier-Stokes equations in the integral form. For the present investigations, the Reynolds averaged Navier Stokes equations (RANS) applying the one-equation Spalart-Allmaras and the two-equation Wilcox k-ω turbulence models were solved. The AUSMDV flux vector splitting scheme is applied together with MUSCL gradient reconstruction to achieve second order spatial accuracy. Different detailed finite rate chemistry models for hydrogen / air combustion were implemented in the TAU code within the LAPCAT project. These are based on previous extensions for chemical and thermal non-equilibrium flows in high enthalpy aerothermodynamics. The flow is considered to be a reacting mixture of thermally perfect gases. The chemical source terms in the corresponding set of transport equations are computed from the law of mass action by summation over all participating reactions. The thermodynamic properties of the individual species are calculated from the partition functions allowing extensions such as multi temperature models to handle thermal non-equilibrium effects. The species diffusion fluxes are modelled using Fick's law applying an averaged diffusion coefficient for all species. Thermal non-equilibrium flows are computed by solving an additional transport equation for the vibrational energy of each molecule in non-equilibrium according to the Milikan and White[12] approach. Further, an assumed Probability-Density-Function (PDF) model as described by Gerlinger[13] was implemented in the DLR Tau code to model the influence of turbulent fluctuations on the species source terms from detailed chemistry schemes. The averaged turbulent chemical source terms are computed by integrating the laminar

expression over all realizable temperatures and species concentrations which are weighted by the probability of their occurrence. These probabilities are given by presumed shape PDFs and additional transport equations for the variance of temperature and the sum of the variances of species concentrations are solved to completely describe the PDF at each point of the flow field.

3.3 Nozzle flow and determination of the free stream conditions in the HEG test section

The evaluation of the free stream conditions in the test section of the HEG free piston driven shock tunnel was based on numerical analysis using a suitable set of measured input parameters. First, the nozzle reservoir conditions were determined performing a 1-dimensional computation of the shock tube flow with ESTC[14]. Based on these nozzle reservoir conditions, the free stream was subsequently determined by numerical computation of the nozzle flow. Different RANS turbulence models were applied in combination with thermal equilibrium and non-equilibrium computations to determine the influence of different modelling assumptions on the obtained free stream conditions. The chemical non-equilibrium 5 species and 17 reactions rate set by Gupta[15] was utilised for this investigation. Previous studies show good performance of this model for chemical relaxation in high enthalpy wind tunnel nozzles. The considered species are molecular and atomic nitrogen and oxygen (N_2, O_2, N, O) and nitric oxide (NO). Numerical results for the Pitot pressure profile (Pt2) at the nozzle exit plane in the HEG test section are shown in the left part of Fig. 5.

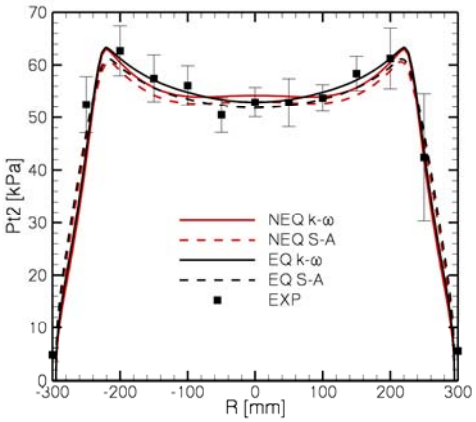

Mach number	[-]	7.20
Temperature	[K]	294
Density	[g/m^3]	10.3
N_2 mass fraction	[-]	0.741
O_2 mass fraction	[-]	0.217
NO mass fraction	[-]	0.041
O mass fraction	[-]	0.001

Figure 5: Pitot pressure profile at the nozzle exit for different models to describe the influence of turbulence and thermal relaxation in the nozzle flow (left) and resulting averaged free stream conditions in the test section (right). (NEQ: thermal non-equilibrium, EQ: thermal equilibrium, S-A: Spalart-Allmaras turbulence model, k-ω: Wilcox k-ω turbulence model, EXP: experiment).

Good agreement is observed between the CFD prediction and the Pitot rake measurements. The shape of the Pitot pressure profile changes with the assumption of thermal equilibrium or non-equilibrium. This is due to different ratios of specific heats in the region downstream of the nozzle throat caused by sudden vibrational freezing, which changes the local Mach number distribution and therefore the characteristics inside the nozzle. The shape of the boundary layer is predicted to be slightly different between the Spalart-Allmaras and the Wilcox k-ω turbulence models. The best agreement with the available experimental data (also the static pressure measurements, not shown here) was achieved with the application of the Wilcox k-ω turbulence model and the assumption of thermal equilibrium.
The free stream conditions of the selected HyShot experiment in HEG were recomputed using the actual nozzle supply total pressure of 6.75 MPa and a total temperature of 2885 K resulting in a total enthalpy of 3.5 MJ/kg. The Wilcox k-ω model and the assumption of thermal equilibrium were applied and the conditions were averaged at the nozzle exit plane between the center line and a radius of 200 mm. The resulting free stream conditions are summarized in the right part of Fig. 5.

3.4. Intake flowfield

The CFD analysis of the HyShot supersonic combustion flight configuration was split into the 2-dimensional investigation of the intake flow and the 3-dimensional analysis of the flow inside the combustion chamber. The intake flow was treated separately in order to minimize the computational effort. An overview of the overlapping computational domains and applied boundary conditions of both the 2D intake and the 3D combustion chamber parts is given in Fig. 6. A detail of the computational grid in the vicinity of the combustion chamber entrance is shown in

the left part of Fig. 7. The unstructured grid was adapted to the resulting shock system. The flow profile along a cut plane as indicated in Fig. 6 at x=360 mm downstream of the leading edge is extracted from the 2D intake solution and then interpolated as a Dirichlet inflow condition to the three dimensional computational grid of the combustion chamber.
The averaged inflow conditions from Fig. 5 were imposed at the farfield boundary. The transition from laminar to turbulent flow on the compression ramp was set at x=280 mm downstream of the leading edge. This transition location corresponds to using a critical Reynolds number of 700,000, which was determined using the measured transition location inside the combustion chamber for fuel-off conditions. The reaction rate scheme of Gupta and the Spalart-Allmaras turbulence model were applied.

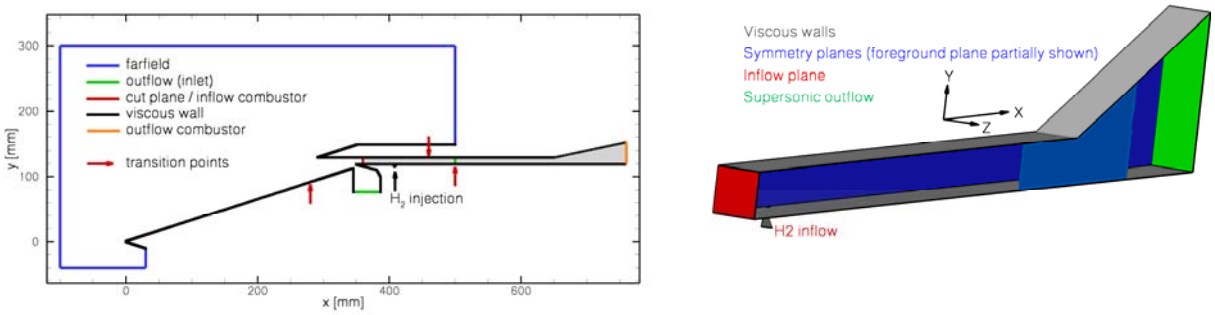

Figure 6: Computational domain and boundary conditions. The three-dimensional domain of the combustion chamber is marked in grey. The locations of transition from laminar to turbulent boundary layers are indicated by the arrows.

A detail of the flow field solution assuming thermal equilibrium is shown in the right part of Fig. 7. The Mach number at the entrance of the rectangular combustion chamber duct is about 2.5. A significant part of the compressed flow is spilled outside the cowl. The entire boundary layer is swallowed by the bleed channel as indicated by the streamlines in Fig. 7. No eddy viscosity, which is generated inside the transitional boundary layer on the compression ramp, enters the combustion chamber. This supports the assumption of applying identical critical Reynolds numbers in the combustor and on the intake ramp.

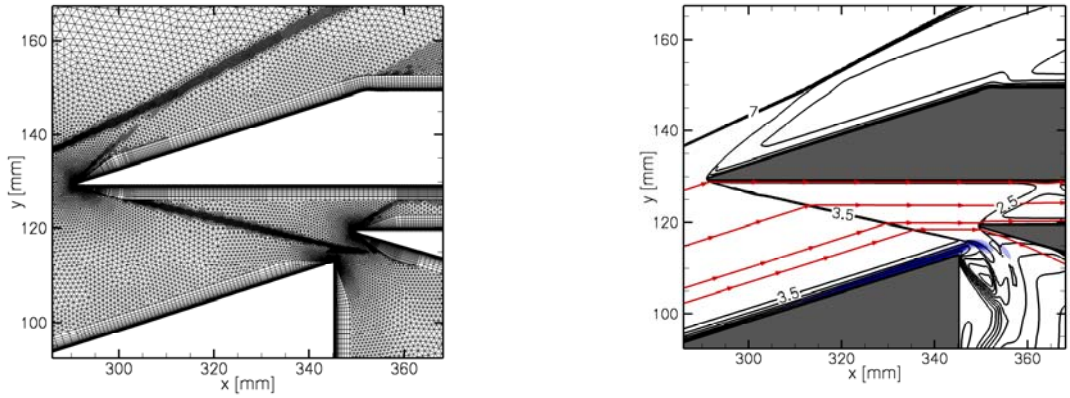

Figure 7: Detail of the CFD grid (left) and detail of the intake flow field (right); black: Mach number isolines, red: streamlines and blue: eddy viscosity contours.

3.5. Combustion Chamber

The flow field inside the HyShot combustion chamber was computed using a 3-dimensional computational domain. The exhaust nozzle was only partially included. All existing symmetries of the flow field are used. An overview of the computational domain and the applied boundary condition is shown in Fig. 6. For better visibility, the plots in Fig. 8 are shown in a scale of x:y:z of 1:2:2.
At the inflow plane at an axial location of x=360 mm downstream of the intake leading edge, the flow profiles obtained from the 2-dimensional intake analysis are prescribed. The supersonic outflow plane is located at x=760 mm. The constant cross section part of the combustor ends at x=650 mm. The height of the combustion chamber in y-direction is 9.8 mm. The width of the HyShot combustor with four equally spaced porthole injectors is 75 mm. Symmetry boundary conditions are used at the spanwise boundary planes. One is located at z=0 mm in the center of a porthole injector. The second symmetry plane is located at z=9.375 mm between two porthole injectors.

Therefore, only one eighth of the original spanwise extension of the HyShot configuration is modelled. Transition from laminar to turbulent flow inside the boundary layers was set at x=500 mm on the bottom wall and x=460 mm at the top wall. This transition location was determined by heat flux measurements and corresponds to a critical Reynolds number of 700,000. The wall temperature is fixed to 300 K accounting for the short test times in the HEG facility. The hydrogen injection was modelled by partially including the injector in the computational domain. A total hydrogen pressure of 2.97 bar and a total temperature of 300 K were prescribed. The computational grid, which covers this domain, consists of 800,000 grid points and was adapted to density, total pressure and temperature gradients. Structured prismatic sublayers were used at the viscous walls. A dimensionless wall spacing of y+=O(1) was used to ensure sufficient resolution for the low Reynolds number turbulence models and for the computation of the wall heat flux. A modified 9 species and 17 steps Jachimowski reaction rate set[13] is applied to the combustor flow. Numerical results show that the penetration of the hydrogen jet is about 30 % of the total combustor height of 9.8 mm. The vortex system, which develops upstream of the injector, efficiently enhances the distribution of hydrogen in the boundary layer of the lower combustor wall. Representative results for the three dimensional flow field are given in Fig. 8 - 10. Contours of hydroxyl mass fraction are shown in the left part of Fig. 8 together with streamlines emanating from the hydrogen porthole injector. The combustion process starts at the shock which is generated by the injected hydrogen jet. A stabilized supersonic flame develops around the hydrogen flow. The hydrogen which is trapped in the boundary layer starts to react close to the injection location.

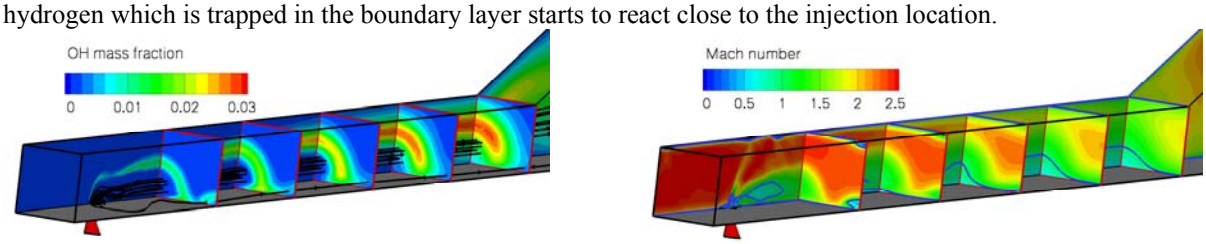

Figure 8: Contours of OH mass fraction and streamlines emanating from the hydrogen injector.

The Mach number contours are plotted in the right part of Fig. 8. The location of the sonic line is also shown in this figure. A small subsonic region develops immediately downstream of the injector. Small separation bubbles are observed at the upper combustor wall upstream of the first cut plane. A large subsonic zone develops further downstream of the combustor. The flow is subsonic over about 10 % of the combustor cross sectional area upstream of the exhaust nozzle.

The pressure distributions on the bottom wall of the combustor along the symmetry line between two injectors are shown in the left part of Fig. 9. The square symbols correspond to the associated HEG measurement with an equivalence ratio of φ=0.43 at an angle of attack of α=3.8 deg. The scatter bars indicate the RMS values of the measured quantities during the test time. The flight data was taken at an altitude of 33 km, an angle of attack of α=3.6 deg and an equivalence ratio of φ=0.30 which was lower than for the wind tunnel experiment. The fuel-off static surface pressure obtained from CFD analysis (Spalart-Allmaras turbulence model) compares well with the wind tunnel experiment.

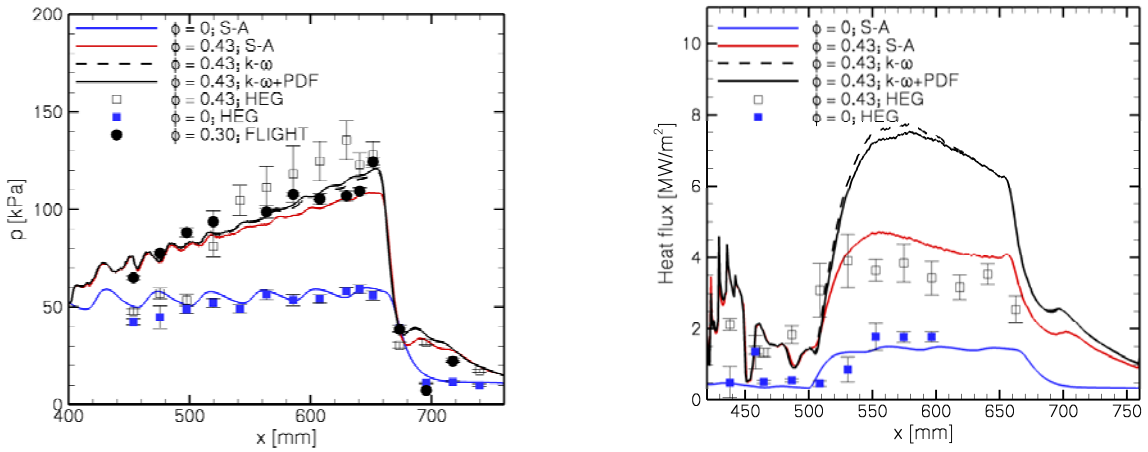

Figure 9: Pressure distribution along the bottom wall of the combustion chamber in the x-y symmetry plane between the hydrogen injectors; (S-A: Spalart-Allmaras turbulence model, k-ω: Wilcox k-ω turbulence model, PDF: assumed PDF for turbulence-chemistry interaction).

Different turbulence models were applied to the fuel-on computations. In the upstream region of the combustor the obtained results are comparable because of the late transition to turbulent boundary layer flow at x=500 mm on the lower combustor wall. In the downstream region of the combustor higher turbulent mixing is predicted by the k-ω model, which leads to a higher level of static pressure upstream of the exhaust nozzle compared to the Spalart-Allmaras model. The application of the assumed-PDF approach for the modelling of turbulence-chemistry interactions leads to a further increase of the achieved pressure level but due to the late onset of turbulence this effect remains small. The difference of the peak pressure levels in the combustor which is due to different turbulence modelling assumptions is about 11 %.
The best agreement to the experimental data is achieved by the Wilcox k-ω turbulence model including assumed PDF. The agreement with the flight data is very good, however, it has to be noted that the flight data corresponds to a significantly lower equivalence ratio. The peak pressure level of 135 kPa that was obtained from the HEG experiments was not reached by any of the CFD simulations which underpredicted this value by 10 to 20 %.
Surface heat flux distributions on the lower combustor wall downstream of the porthole injector are shown in the right part of Fig. 9. Good agreement of the CFD prediction compared to the HEG experiment for both the fuel-on and fuel-off cases is achieved for the application of the Spalart-Allmaras turbulence model. The Wilcox k-ω turbulence model significantly over predicts the measured heat flux levels. The influence of boundary layer transition at x=500 mm is clearly visible in Fig. 9. A significant amount (around 16 %) of the injected hydrogen remains unburned until the end of the combustion chamber.

4. Summary and Conclusions

Within the LAPCAT program the German Aerospace Center, DLR, has conducted several research activities related to supersonic combustion and the development of scramjet engines for sustained flight. The results can be summarized as follows.

The single injector performance experiments revealed that the outer shape of the investigated hydrogen injectors has a distinct influence on the mixing and combustion process inside the model scramjet combustor. Laser diagnostic measurements of the extension of the hydrogen jet delivered indications that for the WAVE injector a more favourable 3-dimensional structure of the hydrogen-air-interface and mixing layer was created, resulting in a noticeably higher heat release in the reacting flow case.

The DLR unstructured/hybrid flow solver TAU was extended for the modelling of the flow path in supersonic combustion ramjet engines. Appropriate models for turbulent hydrogen combustion were implemented. This code was applied to determine the free stream conditions in the HEG test section, to simulate the HyShot intake flow field and for the numerical investigation of the turbulent reacting flow in the combustor. The results presented in this paper correspond to the HEG condition XII which duplicates the HyShot free stream conditions at a flight altitude of 32.5 km. Satisfactory agreement between CFD and experiment was achieved for the static pressure distribution in the combustor by both considered turbulence models and for the surface heat flux distribution by the Spalart-Allmaras model. The CFD analysis confirmed the transition to turbulent boundary layers at 100 mm downstream of the injection location. The numerical analysis of chemically reacting supersonic flows inside scramjet engines is still subjected to uncertainties which are mainly caused by variations in the predictions of the behaviour of boundary and mixing layers obtained by the application of different turbulence models. These uncertainties underline the necessity and urgency of precise validation experiments and of a close link between ground testing, CFD analysis and flight experiments.

Acknowledgement

The work presented was partly financed and performed within the ‘Long-Term Advanced Propulsion Concepts and Technologies’ project investigating high-speed airbreathing propulsion. LAPCAT, coordinated by ESA-ESTEC, is supported by the EU within the 6th Framework Programme Priority 1.4, Aeronautic and Space, Contract no.: AST4-CT-2005-012282. Further info on LAPCAT can be found on http://www.esa.int/techresources/lapcat. The HyShot post flight analysis providing data for LAPCAT was funded by ESA-ESTEC under TRP contract number 17001/02/NL/MV. The M11-4 experiments and parts of the data evaluation were funded by DLR.

Nomenclature

D_{FWHM}	Specifically defined hydrogen jet thickness, [m]
M_{air}	Air flow Mach number, [-]
M_{H2}	H_2 flow Mach number at injector exit, [-]
$\dot{m}_{H2}$	H_2 mass flow rate, [kg/s]
p_s	Wall static pressure, [Pa]
t	Time, [s]
$T_{t,air}$	Air total temperature, [K]
$T_{t,H2}$	H_2 total temperature, [K]
x,y,z	Cartesian coordinates, see Fig. 1, [m]
y+	dimensionless distance from wall
λ	Wavelength, [nm]

Subscripts and abbreviations

EC	Combustor entrance cross section
FWHM	Full width half maximum
Pitot	Pitot
TC1, TC2	Test cases

References

[1] Steelant, J. LAPCAT: A technical feasibility study on sustained hypersonic flight. ISABE-2007-1205, *18th International Symposium on Airbreathing Engines*, September 2007, accepted for presentation.

[2] Paull, A., Alesi, H. and Anderson, S. The HyShot flight program and how it was developed. *AIAA/AAAF 11th International Space Planes and Hypersonic Systems and Technologies Conference*, Orleans, France, 2002.

[3] McClinton, C.R. X-43 – Scramjet power breaks the hypersonic barrier. AIAA-2006-1, Dryden Lectureship in Research for 2006 at the *44th AIAA Aerospace Sciences Meeting and Exhibit*, Reno, Nevada, Jan. 9-12, 2006

[4] Oschwald, M., Guerra, M. and Waidmann, W. Investigation of the flowfield of a scramjet combustor with parallel H_2-injection through a strut by particle image displacement velocimetry. *3rd Int. Symposium on Special Topics in Chemical Propulsion*, 10-14 May 1993, Scheveningen, The Netherlands, in (Proceedings): Non-Intrusive Combustion Diagnostics, (Eds.) K.K. Kuo and T.P. Parr, Begell House, Inc., New York, 1994.

[5] Weisgerber, H., Brummund, U. and Martinuzzi, R. PIV-Messungen in einer Scramjet-Modellbrennkammer. *8. GALA Fachtagung, Proceedings of Lasermethoden in der Strömungsmesstechnik*, 12-14 September 2000, Freising/Weihenstephan, Germany.

[6] Scheel, F. PIV Measurement of a 3-dimensional reacting flow in a SCRAMJET combustion chamber. *42nd AIAA Aerospace Sciences Meeting and Exhibit*, 4-8 January 2004, Reno, NV, USA

[7] Ciezki, H.K., Scheel, F. and Kwan, W. Investigation of the combustion process in a scramjet model combustor with a sampling probe system. AIAA 2004–4166, *40th AIAA Joint Propulsion Conference*, 11–14 July 2004, Fort Lauderdale, FL, USA.

[8] Ciezki, H.K. Determination of concentration and Pitot pressure distributions inside a scramjet model combustor with an intrusive probe system. *EUCASS2007*, 2-6 July 2007, Brussels, Belgium.

[9] Scheel, F., Ciezki, H.K. and Haidn, O.J. Investigation of the influence of streamwise vortices generating geometries of strut injectors on the mixing and combustion process in a scramjet model combustor. *ISABE2007 18th International Symposium on Airbreathing Engines*, September 2007, accepted for presentation.

[10] Gardner, T., Hannemann, K., Paull, A. and Steelant, J. Ground testing of the HyShot supersonic combustion flight experiment in HEG. *Proceedings of the 24th International Symposium on Shock Waves*, Beijing, China, 2004.

[11] Gerhold, T., Friedrich, O., Evans, J. and Galle, M. Calculation of complex three-dimensional configurations employing the DLR-TAU-Code. AIAA-Paper 97-0167, 1997.

[12] Millikan, R.C. and White, D.R. Systematics of vibrational relaxation. *Journal of Chemical Physics*, 39:12:3209-3213, 1963.

[13] Gerlinger, P. An implicit multigrid method for turbulent combustion. *Journal of Computational Physics*, 167:247-276, 2001.

[14] McIntosh, M.K. Computer program for the calculation of frozen and equilibrium conditions in shock tunnels. Australian National University, Canberra A.C.T., 1968.

[15] Gupta, R.N., Yos, J.M., Thompson, R.A. and Lee, K.P. A review of reaction rates and thermodynamic and transport properties for an 11-species air model for chemical and thermal nonequilibrium calculations to 30000 K. NASA Reference Publication, No. 1232, 1990.